Extracting Keplerian signals from noisy data

1995 J. Phys. A: Math. Gen. 28 3269

(http://iopscience.iop.org/0305-4470/28/11/023)

J. Phys. A: Math. Gen. 28 (1995) 3269–3278. Printed in the UK

Extracting Keplerian signals from noisy data

David Lawunmi
Cavendish Laboratory, Madingley Road, Cambridge, CB3 OHE, UK

Received 3 June 1994, in final form 9 November 1994

Abstract. A method for extracting radial velocity signals produced by brown dwarfs and extra solar planets is presented, and the implications of this analysis for the prospects of detecting extra solar planets and brown dwarfs are discussed.

Currently the limiting sensitivity of measurements of stellar radial velocities deduced from the Doppler shift in their spectra is of the order of 5 $m\,s^{-1}$ [1]. Jupiter-mass planets and brown dwarfs that are in binary systems with a primary companion that is visible from Earth (and where the primary star has a mass of the order of or less than one solar mass), are capable of producing perturbations in the radial velocity of their stellar companion that are larger than the current limiting sensitivity of spectral measurements of the radial velocity. In this article the relationship between the orbital dynamics of a binary system consisting of a visible primary star and a companion secondary object (that may be difficult or impracticable to observe directly), and the spectroscopically determined radial velocity of the primary star will be analysed. It is shown that valuable evidence about the nature of low mass secondary objects that are accompanying the primary star may be gleaned from empirical measurements of the radial velocity of the primary gathered over a fraction of the orbital period of the binary system.

It may take the binary system several decades to complete one orbital cycle. Extracting unambiguous information about low-mass secondary components from an analysis of the radial velocity measurements of the primary star is expected to be difficult as velocity variations due to the atmospheric dynamics of the primary may have a similar order of magnitude to the reflex velocity variation induced on the primary star by the secondary object [2].

An earlier study of the fractional orbit problem and its application to analysing the orbital dynamics of binary systems was undertaken by Monet [3]; however, most of the methods for analysing radial velocity data that are currently being used to check for the presence of low-mass secondary objects rely on data being collected over one or more orbital cycles [2, 4, 5]. If a data analysis technique can provide information about the presence of a secondary object by using data from a fraction of an orbital cycle, it is potentially of great value as it could save several years of observing time.

In addition to the analysis of the radial velocities of primary stars, a wide variety of other methods for detecting secondary objects in binary systems are also being implemented and developed. These include astrometric methods, gravitational microlensing, and direct observation, [1, 2, 6–9].

The orbits of the primary star and the secondary object with respect to their barycentre were determined by analysing the dynamics of the binary system in terms of the two-body

0305-4470/95/113269+10$19.50

problem [10]. The radial velocity of the primary star with respect to the observer of the binary system, v^*, is given by the expressions [11, 12],

$$v^* = K\,(e\cos(\tilde{\omega}) + \cos(f + \tilde{\omega})) + \gamma \tag{1a}$$

$$K = \left(\frac{m_s}{m_s + M^*}\right)\left(\frac{\mu}{a\left(1 - e^2\right)}\right)^{1/2} \sin(i) \tag{1b}$$

$$\mu = G\left(m_s + M^*\right) \tag{1c}$$

where m_s is the mass of the secondary body; $M*$ is the mass of primary star; a is the semi major axis of the secondary with respect to the primary star; e is the eccentricity of the similar orbits of the primary star and the secondary object with respect to their barycentre; f is the true anomaly; i is the inclination of the orbit; $\tilde{\omega}$ is the argument of periastron; and γ is the contribution to the radial velocity of the primary that results from the proper motion of the binary system.

Information about the nature of the orbital motion of the primary star with respect to the barycentre of a binary system can be obtained by taking advantage of some of the mathematical properties of periodic orbital motion on an elliptical path. For the purposes of the mathematical approach adopted in this article, it is convenient to express the radial velocity of the primary star as

$$V^*_{\text{meas}} = V^*_{\text{per}} + V^*_{\text{noise}} + V^*_{\text{const}} \tag{2}$$

where the measured radial velocity has been split into three terms, the periodic contribution due to the reflex radial velocity due to the secondary object perturbing the primary object $V^*_{\text{per}} = K\cos(f + \tilde{\omega})$, a noise term and a constant term $Ke\cos(\tilde{\omega}) + \gamma$.

The velocity V^*_{meas} can be expressed as:

$$V^*_{\text{meas}} = a_1\cos(f) + b_1\sin(f) + V^*_{\text{noise}} + V^*_{\text{const}}. \tag{3}$$

The limiting values of the true anomaly that define the data that is under analysis are represented by $x_{\min} \leqslant f \leqslant x_{\max}$. The time interval between the data points was not uniform, in this study it was obtained by dividing the interval $x_{\min} \leqslant f \leqslant x_{\max}$ into uniform sub-intervals and adding a random number that could take on any value between zero and 90% of the size of a subinterval to the point at the beginning of the subinterval. The radial velocity noise was modelled by a random number generator; for the analysis given in tables 1, 3 and 4 it has a normal probability distribution function given by:

$$P(x) = \left[\frac{1}{b\sqrt{2\pi}}\right]\exp\left[\frac{(x-\sigma)^2}{2b^2}\right] \tag{4}$$

where σ is the mean of the distribution and b is the standard deviation of the distribution. The noise in table 2 was modelled by a uniform probability distribution function.

The contribution to the integral corresponding to a_1 in equation (5) from a noisy set of data, for $x_{\min} \leqslant f \leqslant x_{\max}$, is calculated and compared with the corresponding contribution from data that is free from noise, for a number of different values of $x_{\min}$ and $x_{\max}$, in tables 1–3. These estimates were obtained by utilizing the expression

$$a_1 \approx I = \frac{\int_{x_{\text{LL}}}^{x_{\text{UL}}} (v^*(f)) - v^*_{\min})\cos(f)\,\mathrm{d}f}{\frac{1}{2}\,(x_{\text{UL}} - x_{\text{LL}}) + \frac{1}{4}\,[\sin(2x_{\text{UL}}) - \sin(2x_{\text{LL}})]}.$$

Table 1. The secondary object is a Jupiter-mass planet, the primary object is a star with a mass equal to one solar mass, $e = 0.1$, $T = 12$ years; noise is normally distributed, $b = 10\ \mathrm{m\,s^{-1}}$, $\sigma = 10^5\ \mathrm{m\,s^{-1}}$, $\tilde{\omega} = \frac{\pi}{6}$.

a_1 Noisy data $\mathrm{m\,s^{-1}}$	a_1 Noise-free data $\mathrm{m\,s^{-1}}$	$x_{\min}, x_{\max}$
48.29	14.78	$0, \frac{\pi}{2}$
13.35	10.80	$\frac{\pi}{4}, \frac{3\pi}{4}$
−34.21	6.83	$\frac{\pi}{2}, \pi$
−44.47	10.80	$\frac{3\pi}{4}, \frac{5\pi}{4}$
−44.30	14.78	$\pi, \frac{3\pi}{2}$
11.30	10.80	$\frac{5\pi}{4}, \frac{7\pi}{4}$
44.82	6.83	$\frac{3\pi}{2}, 2\pi$
30.85	10.80	$\frac{7\pi}{4}, \frac{9\pi}{4}$

Table 2. The secondary object is a Jupiter-mass planet, the primary object is a star with a mass equal to one solar mass, $e = 0.1$, $T = 12$ years, the noise is uniformly distributed between $-10\ \mathrm{m\,s^{-1}}$ and $10\ \mathrm{m\,s^{-1}}$, $\tilde{\omega} = \frac{\pi}{6}$.

a_1 Noisy data $\mathrm{m\,s^{-1}}$	a_1 Noise-free data $\mathrm{m\,s^{-1}}$	$x_{\min}, x_{\max}$
17.74	14.78	$0, \frac{\pi}{2}$
9.85	10.80	$\frac{\pi}{4}, \frac{3\pi}{4}$
−19.83	6.83	$\frac{\pi}{2}, \pi$
−13.91	10.80	$\frac{3\pi}{4}, \frac{5\pi}{4}$
−13.26	14.78	$\pi, \frac{3\pi}{2}$
10.95	10.80	$\frac{5\pi}{4}, \frac{7\pi}{4}$
26.84	6.83	$\frac{3\pi}{2}, 2\pi$
15.27	10.80	$\frac{7\pi}{4}, \frac{9\pi}{4}$

x_{UL} and x_{LL} are quasi-symmetric points about a point of odd symmetry of $\cos(f)$, and $v^*_{\min}$ is the smallest value of the radial velocity in the data series. The expression defined as I should be equal to the expansion coefficient a_1, when the contribution of the noise to the measured radial velocity is zero and the points x_{UL} and x_{LL} are equidistant from the appropriate point of odd symmetry of $\cos(f)$. All of the integrals in tables 1, 2 and 3 used 201 points inclusive of the two end points, $x_{\min}$ and $x_{\max}$.

The reflex radial velocity data in this study was generated by using equations (1*a*), (1*b*) and (1*c*). A graph illustrating the simulated data and the observations is shown in figure 1. Estimates of the coefficient a_1 in equation (3) from a noisy set of data, for $x_{\min} \leqslant f \leqslant x_{\max}$, are compared with the corresponding contribution from data that is free from noise, for a number of different sets of values of $x_{\min}$ and $x_{\max}$, in tables 1–3.

In (3),

$$a_1 = K\cos(\tilde{\omega}) \tag{5}$$

$$b_1 = -K\sin(\tilde{\omega}) \tag{6}$$

The values of the standard deviation and the mean of the noise of the radial velocity data can have a significant effect on the quality of the information that can be extracted from the data. The effects of the mean were mitigated by subtracting the smallest value of

Table 3. The secondary object is a brown dwarf, the primary object is a star with a mass equal to one solar mass. The mass of the secondary object is 5% of the mass of the Sun, $e = 0.1$, $T = 12$ years; noise is distributed according to the normal probability distribution function, $b = 10\ \mathrm{m\,s^{-1}}$, $\sigma = 10^5\ \mathrm{m\,s^{-1}} = \frac{\pi}{6}$.

a_1 Noisy data $\mathrm{m\,s^{-1}}$	a_1 Noise-free data $\mathrm{m\,s^{-1}}$	$x_{\min}$, $x_{\max}$
370.74	749.53	$0, \frac{\pi}{2}$
550.64	548.08	$\frac{\pi}{4}, \frac{3\pi}{4}$
−356.61	346.63	$\frac{\pi}{2}, \pi$
−187.57	548.08	$\frac{3\pi}{4}, \frac{5\pi}{4}$
−86.97	749.53	$\pi, \frac{3\pi}{2}$
548.59	548.08	$\frac{5\pi}{4}, \frac{7\pi}{4}$
744.23	346.63	$\frac{3\pi}{2}, 2\pi$
357.46	548.08	$\frac{7\pi}{4}, \frac{9\pi}{4}$

Table 4. *In this table the the integral I (see (7) is calculated and displayed. The data set* comprised of 201 radial velocity points obtained between the true anomaly values $f = \frac{5\pi}{4}$ and $f = \frac{7\pi}{4}$. Thirty three integrals where the upper and the lower limits were almost symmetrical with respect to the true anomaly point $f = \frac{3\pi}{4}$ were obtained. The minimum separation between the upper limit and the symmetry point and the lower limit of the integral and the symmetry point was chosen to be $\frac{\pi}{6}$. Points closer to the symmetry point than this were not used in order that the integral was taken over a sufficiently large sample of data points. The true value of a_1 corresponding to the input data is: $a_1 = 10.80\ \mathrm{m\,s^{-1}}$. The orbital parameters of the secondary object and the noise distribution function are the same as those in table 1.

a_1 estimate $\mathrm{m\,s^{-1}}$	a_1 estimate $\mathrm{m\,s^{-1}}$	a_1 estimate $\mathrm{m\,s^{-1}}$	a_1 estimate $\mathrm{m\,s^{-1}}$
10.28	10.47	10.65	11.63
9.88	9.06	10.91	11.47
9.33	10.38	10.54	11.17
11.63	11.40	10.68	11.33
10.31	10.44	11.18	11.68
11.11	10.43	11.06	12.10
10.28	10.51	11.36	
11.48	9.94	11.72	
12.01	10.36	11.36	

the data sample from all of the data points before determining the values of the expansion coefficients a_1 and b_1 in equation (3). The discrepancy between the ideal case which corresponds to zero noise, and the contribution to a_1 and b_1 from noisy radial velocity data tends to increase with the standard deviation of the noisy data.

If radial velocity data is symmetrically distributed about a point of odd symmetry of $\cos(f)$ then the noise free data series can be related to the component of the radial velocity that is due to the influence of the gravitational attraction of the secondary object on the primary object.

$$I = \frac{\int_{x_{\mathrm{LL}}}^{x_{\mathrm{UL}}} (v^*(f)) - v^*_{\min}) \cos(f)\,\mathrm{d}f}{\frac{1}{2}(x_{\mathrm{UL}} - x_{\mathrm{LL}}) + \frac{1}{4}[\sin(2x_{\mathrm{UL}}) - \sin(2x_{\mathrm{LL}})]}. \tag{7}$$

Similarly, when one has a noise-free data series that is symmetrically distributed about $\sin(f)$,

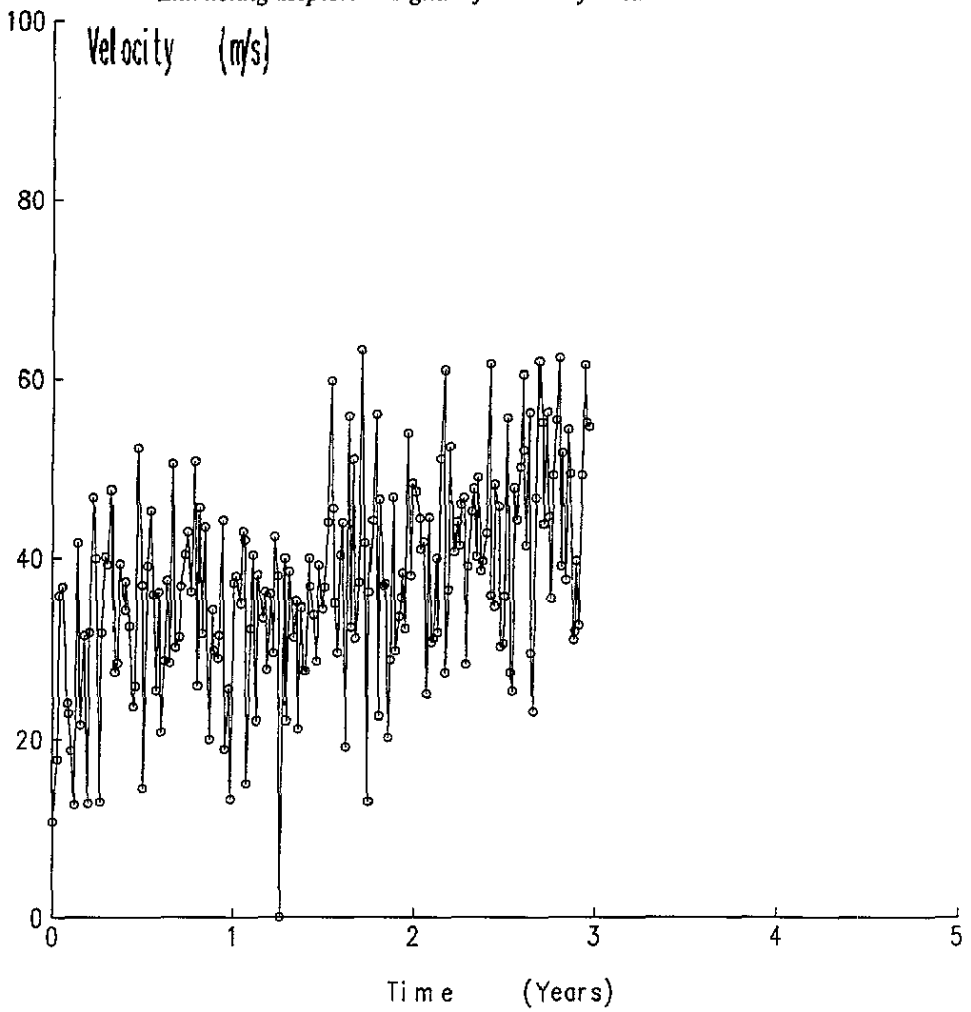

Figure 1. In this figure the difference between the radial velocity of the primary star and the smallest radial velocity of the primary in the data series is illustrated. The circles illustrate the times at which the spectrum of the primary star was analysed.

$$J = \frac{\int_{x_{LL}}^{x_{UL}} (v^*(f)) - v^*_{min}) \sin(f)\, df}{\frac{1}{2}(x_{LL} - x_{UL}) + \frac{1}{4}[\sin(2x_{UL}) - \sin(2x_{LL})]} \tag{8}$$

where

$$I = K \cos(\tilde{\omega}) \tag{9}$$

and

$$J = -K \sin(\tilde{\omega}) \tag{10}$$

and v^*_{min} is the smallest velocity in the data set that is being analysed.

The above expressions for I and J are exact when the noise is zero and x_{UL} and x_{LL} are distributed symmetrically with respect to the relevant point of odd symmetry of $\cos(f)$ and $\sin(f)$ respectively. In practice the points x_{UL} and x_{LL} will generally not be equidistant from

the point of odd symmetry of the sin or the cos function and there will also be noise in the radial velocity data. If the pairs of quasi-symmetric points are close to being symmetrically distributed about a point of odd symmetry of the $\sin(f)$ or $\cos(f)$, the expressions for I and J will generally yield a reasonable estimate of the integral obtained from noisy data, even in situations where the contribution from the noise to the radial velocity is much greater than that from the periodic perturbation in the radial velocity of the primary object with respect to the observer due to the secondary object, as illustrated in table 4 and figure 1. Generally, when analysing radial velocity data to ascertain if a secondary object is present, the observer will not have any *a priori* information about the orbital parameters of the secondary object. In order to overcome this problem, the orbital parameters can be treated as variable parameters and their values can be varied over a wide range of possible solution sets. This can be achieved by varying the values of the initial value of the true anomaly, f_0, the orbital period of the system T and the orbital eccentricity of the system, e, and evaluating the integral I or J corresponding to this set of parameters. The true anomaly corresponding to data points that were obtained after the initial point can be obtained by utilising the values of f_0, e and T in conjunction with the following equations

$$\tan\left(\frac{f}{2}\right) = \left(\frac{1+e}{1-e}\right)^{1/2} \tan(E/2) \tag{11}$$

where f is the true anomaly and E is the eccentric anomaly;

$$M = E - e\sin(E) \tag{12}$$

where M is the mean anomaly at time t_0.

The relationship between M the orbital period T, the time t, and the time that corresponds to the initial data point t_0 is given by:

$$M - M_0 = \left(\frac{2\pi}{T}\right)(t - t_0). \tag{13}$$

Generally the values of the integrals I and J when evaluated over a number of pairs of quasi-symmetrical points distributed about a point of odd symmetry of $\cos(f)$ or $\sin(f)$ will have a wide range for a given potential solution set of the orbital parameters, (f_0, e, T). When the solution set is close in value to that of the orbital parameters of the binary system the spread in the values of the integrals I or J will tend to be much smaller than the corresponding spread in the values of these integrals generated from a set of orbital parameters that are not close to those of the binary system. The candidate orbital parameters of the binary system can be checked for consistency by comparing these parameters with the solution set of orbital parameters that are obtained from radial velocity data, which includes observations subsequent to those that were initially used to determine the orbital parameters of the binary system.

A noise analysis scheme can be implemented in order to determine the probability that any 'Keplerian signature' is due to a secondary companion to the primary star. This can be achieved by comparing the noise in the empirical radial velocity data with random noise generated from a probability distribution function that produces variations of a similar nature and magnitude to the empirical radial velocity noise, and then calculating the contribution to the coefficient a_1, and or b_1 that results purely from the random noise. This method of noise analysis can provide a means of estimating the false alarm probability. If the values of a_1, and or b_1 that are generated entirely by the noise are generally significantly smaller

than those that are obtained from an analysis of some radial velocity data, we have strong evidence in favour of a secondary object. This scheme is illustrated in figure 2 where the noise probability was generated from a normal distribution with a standard deviation of $10\,\mathrm{m\,s^{-1}}$ and a mean of $10^5\ \mathrm{m\,s^{-1}}$. The results from this noise analysis can be appreciated by comparing the coefficients obtained from the random noise with those in table 4. Analysis of the values of a_1 produced by the random noise demonstrates that the probability of producing coefficients of the order of magnitude of those in table 4 from random noise is relatively small.

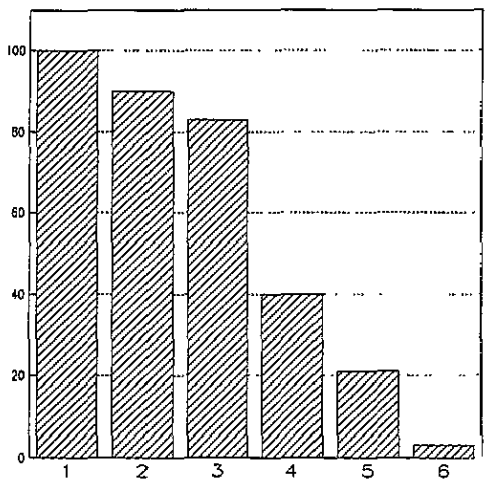

Figure 2. This histogram analyses the absolute magnitude of 337 data values of expansion coefficients generated from normally distributed noise with $b = 10\ \mathrm{m\,s^{-1}}$, $\sigma = 10^5\ \mathrm{m\,s^{-1}}$. It demonstrates the relative probabilities of the noise-making contributions to the first-order expansion coefficients. Studies of the contribution of the noise to the first-order expansion coefficients using sets of data points that had a higher degree of symmetry in their quasi-symmetric points about the appropriate point of odd symmetry demonstrated that the probability of the noise contributing significantly to the first-order expansion coefficients can be reduced by a significant factor by increasing the degree of symmetry between the quasi-symmetric points. The integrals that generated the expansion coefficients a_1 were obtained by using the lower limit, $f = \frac{5\pi}{4}$ and the upper limit, $f = \frac{7\pi}{4}$. In column (1) $0 \leqslant |a_1| < 1$; in column (2) $1 \leqslant |a_1| < 2$; in columns (3)–(5) the range of values of the modulus of the coefficient a_1 can be determined by adding unity to both the upper and the lower limits of the preceding column. The final column, column (6), represents the values of $|a_1|$ when $|a_1| \geqslant 5$.

In principle the argument of periastron, $\tilde{\omega}$, can be determined when there is sufficient radial velocity data about a point of odd symmetry corresponding to only one of the expansion coefficients a_1 or b_1. Another set of expansion coefficients can be obtained by utilising pairs of quasi-symmetric points about a point of odd symmetry of $\cos(f + \beta)$. The angle β is chosen so that there is sufficient radial velocity data to undertake an analysis about points with a true anomaly given by $f = (2n + 1)\frac{\pi}{2} - \beta$.

Initially one would generally expect points of odd symmetry of $\cos(f + \beta)$ to be very close to those of either $\cos(f)$ or $\sin(f)$. However, as the size of the data series increases with time, one will ultimately be able to utilise a larger range of values of β. The relationship between the first-order expansion coefficients that have $f = (2n + 1)\frac{\pi}{2}$ as a point of odd

symmetry, a_1, and the coefficient determined by analysing quasi symmetric points about $f = (2n+1)\frac{\pi}{2} - \beta$, $a_{\beta 1}$, is given by

$$a_{\beta 1} = a_1 \cos(\beta) - b_1 \sin(\beta) \tag{14}$$

hence determining the coefficient $a_{\beta 1}$ provides information that enables one to estimate b_1 and $\tilde{\omega}$. The argument of periastron may be estimated by obtaining a set of first-order expansion coefficients about the point of odd symmetry, $f = (2n+1)\frac{\pi}{2} - \beta$, and a set of expansion coefficients about the point of odd symmetry $f = (2n+1)\frac{\pi}{2}$, and then calculating the range in argument of periastron that these two sets of coefficients yield. This process is illustrated in the histogram in figure 3. The modal according to this analysis is in the range $\frac{\pi}{9} \leqslant \tilde{\omega} \leqslant \frac{5\pi}{36}$. The true value of $\tilde{\omega}$ is $\tilde{\omega} = \frac{\pi}{6}$. The noise in the radial velocity data generally has a stronger effect on the argument of periastron than it has on the expansion coefficients from which this angle is determined. This is probably due to the effects of combining the noise from both sets of data to obtain. Despite the noise, values of β can be determined that should allow one to make a reasonable estimate of the mass function with the above method; this is illustrated in table 5.

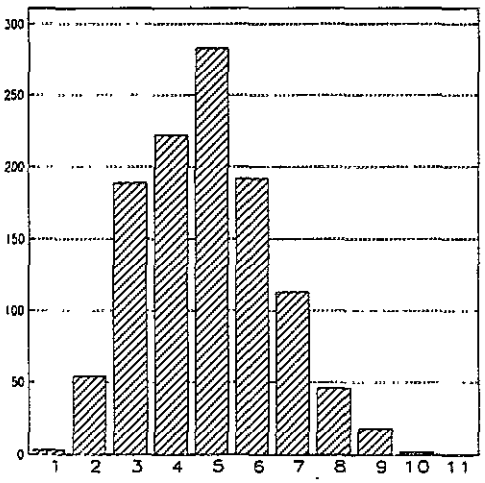

Figure 3. This histogram analyses the argument of periastron generated from the expansion coefficients $a_{\beta 1}$ and a_1. In column (1) $0° \leqslant \tilde{\omega} < 5°$; in column (2) $5° \leqslant \tilde{\omega} < 10°$; for the next eight columns the range in the values of can be determined by adding 5° to both the upper and the lower limits of the preceding column. The final column represents values of $\tilde{\omega}$ when $\tilde{\omega} \geqslant 50°$.

Evidence supporting the presence of a low-mass secondary object can be obtained by undertaking an analysis of high-precision radial velocity data. A fit for the eccentricity, the orbital period and f_0 can be obtained by varying these parameters and analysing the behaviour of the resulting contributions to the expansion coefficients. (In practice, when analysing the data from the various candidate orbits, the spread in the values of the expansion coefficients is expected to be relatively small when one has estimates of these parameters that are close to the true values.) One can also obtain orbital parameters by using additional data from later observational studies of the primary star. The sets of parameters derived by utilising this new data can be compared with orbital parameters obtained from data sets

Table 5. This table illustrates the orbital parameters that were deduced from the simulated radial velocity data. The true orbital parameters are the same as those in table 4. Note there are two possible values for the initial true anomaly; both values are equidistant from each of the two points of odd symmetry of the $\cos(f)$ function for $0 \leqslant f \leqslant 2p$. The mass function, $\Xi(m)$ can be calculated by using the expression $\Xi(m) = m_s^3 (m_s + M^*)^{-2} \sin^3 i = K^3 (1 - e^2)^{3/2} (T/(2\pi G))$. The mass function was found to lie in the range 4.82×10^{20} Kg $\leqslant \Xi(m) \leqslant 3.04 \times 10^{21}$ Kg. The correct value of $\Xi(m)$ is: $\Xi(m) = 1.73 \times 10^{21}$ Kg.

Period	12 ± 0.5 years
Argument of periastron	$\frac{\pi}{8} \pm \frac{2\pi}{36}$
Number of observations	201
Orbital half amplitude, K	11.99 ± 2.79 ms^{-1}
Eccentricity	0.1 ± 0.1
Initial true anomaly, f_0	$\frac{5\pi}{4} \pm 0.032^c$, $\frac{\pi}{4} \pm 0.032^c$

based on earlier data and checked for consistency. By combining the information from the noise analysis and the subsequent motion of the primary star, a decision can be made about the likelihood that the primary star is accompanied by a low-mass secondary object.

The mass of the secondary component of the binary system cannot be unambiguously determined merely by measuring the radial velocity of the primary star, as the angle of inclination of the orbit of the binary system is not divulged from the spectroscopic analysis of the radial velocity of the primary star. There are thus a range of masses that correspond to the radial velocity data of the primary object. This ambiguity may however be alleviated and the mass of the secondary companion can be constrained if it is possible to undertake a high resolution spectral analysis of the effects of the rotation of the primary star on its absorption line profiles [13–15].

In summary, it has been shown that it is feasible to use noisy radial velocity data from a fraction of an orbital cycle in order to check for the presence of a low-mass companion to a bright primary star. The analysis presented in this article should be useful in the field of cosmogony and should also complement observational searches for brown dwarfs and extra solar planets, e.g. the high precision work of McMillan *et al* [16]. The techniques developed in this study should also be useful for analysing the effects of extra solar planets and brown dwarfs on the proper motion of the primary star [17].

Acknowledgments

I would like to thank Dr Bob McMillan and Dr Dave Monet for introducing me to some of the work that is referenced in this article and for their trenchant criticisms of some earlier drafts of this article. I would also like to express my gratitude to Miss Margaret Carlton, Professor Volker Heine and Dr Mike Payne for their support and encouragement.

References

[1] Sargent A I and Beckwith S V W 1993 *Phys. Today* (April) p 22
[2] Burke B *et al* 1993 *TOPS: Toward Other Planetary Systems* US GPO Jacket No 327-494 (Alexandria, VA: De Lancey)
[3] Monet D G 1979 *Astrophys. J.* **234** 275
[4] Horne J H and Baliunas S L 1986 *Astrophys. J.* **302** 757
[5] Scargle J D 1982 *Astrophys. J.* **263** 835
[6] Burrows A and Liebert J 1993 *Rev. Mod. Phys.* **65** 301

[7] Stevenson D J 1991 *Annual Rev. Astron. Astrophys.* **29** 163
[8] Black D C 1980 *Space Rev.* **25** 35
[9] Gatewood G D 1987 *Astron. J.* **94** 213
[10] Roy A E 1988 *Orbital Motion* (Bristol: Institute of Physics) ch 4 and 14
[11] Aitken R G 1935 *The Binary Stars* (New York: McGraw Hill)
[12] Heintz W D 1978 *Double Stars* (Dordrecht: D Reidel)
[13] Cochran W D, Hatzes A P and Hancock T J 1991 *Astrophys. J.* **380** L35
[14] Dravins D 1987 *Astronomy Astrophys.* **172** 200
[15] Dravins D and Nordlund A 1990 *Astronomy Astrophys.* **228** 203
[16] McMillan R S, Moore T L, Perry M L and Smith P H 1993 *Astrophys. J.* **403** 801
[17] Lawunmi D 1995 (to be submitted)